

$O(N)$ algorithms for disordered systems

V. E. Sacksteder*

*Vecchio Edificio Marconi, Dipartimento di Fisica,
Università degli Studi di Roma "La Sapienza,"
P. Aldo Moro 2, 00185 Roma, Italy*

SUMMARY

The past twelve years have seen the development of many algorithms for approximating matrix functions in $O(N)$ time, where N is the basis size. These $O(N)$ algorithms rely on assumptions about the spatial locality of the matrix function; therefore their validity depends very much on the argument of the matrix function. In this article I carefully examine the validity of certain $O(N)$ algorithms when applied to hamiltonians of disordered systems. I focus on the prototypical disordered system, the Anderson model. I find that $O(N)$ algorithms for the density matrix function can be used well below the Anderson transition (i.e. in the metallic phase;) they fail only when the coherence length becomes large. This paper also includes some experimental results about the Anderson model's behavior across a range of disorders.

Copyright © 2000 John Wiley & Sons, Ltd.

KEY WORDS: matrix functions; linear scaling; order N ; basis truncation; Goedecker algorithm; Chebyshev polynomial; Anderson model; localization; coherence length; matrix dot product

1. INTRODUCTION

Certain matrix functions - the Green's function, the density matrix, and the logarithm - are very important to science and engineering. Where they are important, scientists are faced with a computational bottleneck: evaluation of a matrix function generally requires $O(N^3)$ time, where N is the basis size and usually scales linearly or worse with the system volume. This prohibits computations of large systems, even with modern computers. In particular, if a matrix function must be recalculated at every step of a system's evolution in time, then calculations with a basis size larger $O(1000 - 10000)$ are not practical.

In 1991 W. Yang introduced the Divide and Conquer algorithm, which approximated a matrix function in $O(N)$ time[21]. This stimulated the development of many other $O(N)$ algorithms [1, 2, 11] which have met considerable success, permitting for instance quantum dynamics calculations of tens of thousands of atoms. All $O(N)$ algorithms rely on special characteristics of the system under study, and the question of their validity can be answered

*Correspondence to: vincent@sacksteder.com

only after having specified that system. To date, theoretical studies of the validity of these algorithms have occurred almost exclusively within the conceptual framework of ordered systems, using ideas of metals, insulators, and band gaps[6, 7, 8, 9, 10, 11, 12, 13, 14, 15]. In this paper I carefully examine the applicability of $O(N)$ algorithms to disordered systems. I calculate a matrix function two ways: with an $O(N)$ algorithm, and via diagonalization. Comparison of the two results provides some new insight into when disorder can make $O(N)$ calculations feasible.

The format of this paper is as follows: I begin with two introductions: to $O(N)$ algorithms (section 2,) and to a particular matrix function: the density matrix (section 3.) Section 4 offers several rough estimates of the error incurred by $O(N)$ algorithms, while section 5 discusses the metrics I use in my measurements. I present my numerical results in section 6, and finish in section 7 with a short assessment of their reliability.

2. O(N) Algorithms

All $O(N)$ algorithms make three basic assumptions:

- Existence of a Preferred, Local Basis. It is assumed that the system is best described in terms of a localized basis set. I define a basis as localized if for any position \vec{x} , only a small number of basis elements $|\psi\rangle$ satisfy $\langle\vec{x}|\psi\rangle \neq 0$.
- Existence of a Distance Metric. There must be a way of computing the physical distance between any two eigenvectors $|\psi\rangle$ and $|\tilde{\psi}\rangle$.
- Locality of both the Matrix Function and its Argument. I call a matrix A local if, for every pair of basis elements $|\vec{x}\rangle$ and $|\vec{y}\rangle$ that are far apart, $\langle\vec{x}|A|\vec{y}\rangle = 0$. Throughout this article I choose a simple criterion for being far apart: comparison with a radius R .

There are a number of ways for an $O(N)$ algorithm to exploit the three basic assumptions. In this article I focus on the class of algorithms based on basis truncation. This class includes Yang's Divide and Conquer algorithm[21], the "Locally Self-Consistent Multiple Scattering" algorithm[3, 4], and Goedecker's "Chebychev Fermi Operator Expansion"[22, 23], which I will henceforth call the Goedecker algorithm. Basis truncation algorithms break the matrix function into spatially separated pieces. Given the position of a particular piece, the basis is truncated to include only elements close to that position, and then the matrix function is calculated within the truncated basis. Thus, for any generic matrix function $f(H)$, a basis truncation algorithm calculates $\langle\vec{x}|f(H)|\vec{y}\rangle = \langle\vec{x}|f(P_{\vec{x},\vec{y}}HP_{\vec{x},\vec{y}})|\vec{y}\rangle$, where $P_{\vec{x},\vec{y}}$ is a projection operator truncating all basis elements far from \vec{x} , \vec{y} . There may be also an additional step of interpolating results obtained with different P 's, but I will ignore this. In this paper I choose P to be independent of the left index \vec{x} , and to truncate all basis elements outside a sphere of radius R centered at \vec{y} .

Given choices of which matrix function to evaluate, of how to break up the function, of which projection operator to use, and of a possible interpolation scheme, all basis truncation algorithms should converge to identical results. Moreover, given an identical choice of matrix function, variations in the other choices should obtain results that are qualitatively the same. In this paper I use the Goedecker algorithm, but I want to emphasize that the results obtained here apply to the whole class of basis truncation algorithms.

The Goedecker algorithm is essentially a Chebyshev expansion of the matrix function. As long as all the eigenvalues of the argument H are between 1 and -1 , a matrix function may be expanded in a series of Chebyshev polynomials of H : $f(H) \cong \sum_{s=0}^S c_s T_s(H)$. The coefficients c_s are independent of the basis size, and therefore can be calculated numerically in the scalar case. The Chebyshev polynomials can be calculated in $O(N)$ time using the recursion relation $T_{s+1} = (2HT_s) - T_{s-1}$, $T_1 = H$, $T_0 = 1$. (Of course, one must also bound the highest and lowest eigenvalues of H and then normalize. In practice very simple heuristics are sufficient for estimating these bounds.) If the matrix function $f(H)$ has a characteristic scale of variation α , then the error induced by the Chebyshev expansion is controlled by an exponential with argument of order $-\alpha S$.

3. The Density Matrix

In this paper I restrict my attention to a single matrix function, the density matrix. This function is very important in quantum calculations of electronic structure in atoms and molecules, where its argument is the system's Hamiltonian, its diagonal elements describe the charge density, and its off-diagonal elements are used to compute forces on the atoms. Eigenvalues of the Hamiltonian give the energies of their corresponding electronic states, and I will use the words eigenvalue and energy interchangeably throughout the rest of this paper.

The density matrix function $\rho(\mu, T, H)$ is basically a projection operator which deletes eigenvectors having energy E larger than the Fermi level μ . Here I use the following form:

$$\rho(\mu, T, H) = \frac{1}{2} \operatorname{Erfc}\left(\sqrt{2}\left(\frac{H - \mu}{T}\right)\right)$$

For physical reasons, it is not quite a projection operator: it has a transition region around μ of width proportional to the temperature T where its eigenvalues interpolate between 0 and 1. The error induced by a Chebyshev expansion is controlled by an exponential with argument proportional to $-TS/\Delta$, where Δ is the size of the energy band and S is the number of terms in the Chebyshev expansion[22].

The density matrix is well suited to $O(N)$ algorithms. As μ becomes large, it converges to the identity. Moreover, it is invariant under unitary transformations acting on the set of eigenvectors with energies below the Fermi level[2]. Even when the Hamiltonian's eigenvectors are not a local basis set, often a unitary transformation can be found which maps them to a basis which is localized. If such a transformation exists, the density matrix is localized.

Several papers have examined density matrix locality in the context of ordered systems; i.e. ones whose Hamiltonians possess lattice translational invariance[6, 7, 8, 9, 10, 11, 12, 13, 14, 15]. (Lattice translational invariance can be expressed quantitatively as $\langle \vec{x} | H | \vec{y} \rangle = \langle \vec{x} + \vec{\Delta} | H | \vec{y} + \vec{\Delta} \rangle$ for all $\vec{\Delta}$ located on an infinitely extended lattice.) It is well known that the eigenvalues of such systems are arranged in bands separated by energy gaps where there are no eigenvalues, and that the eigenvectors are extended through all space. Notwithstanding the nonlocality of the eigenvectors, there are strong arguments for localization in all ordered systems. If the system is metallic (meaning that the Fermi level lies in one of the bands of eigenvalues) and the temperature is zero, then in a three-dimensional system the density matrix is expected to fall off asymptotically as R^{-2} , where R is the spatial distance from the diagonal. A non-zero temperature multiplies this by an exponential decay. If instead the system is an insulator, then the density matrix should decay exponentially even at $T = 0$.

Most systems of physical interest do not exhibit lattice translational symmetry. In particular, many exhibit inhomogeneities at scales much smaller than that of the system itself. These are termed disordered systems. In this article I study the prototypical disordered system, the Anderson model[18]. It describes a basis laid out on a cubic lattice, one basis element per lattice site, and a very simple symmetric Hamiltonian matrix H composed of two parts:

- A regular part: $\langle \vec{x}|H|\vec{y} \rangle = 1$ if \vec{x} and \vec{y} are nearest neighbors on the lattice. This term is, up to a constant, just the second order discretization of the Laplacian; its spectrum consists of a single band of energies between $-2D$ and $2D$, where D is the spatial dimensionality of the lattice.
- A disordered part: Diagonal elements $\langle \vec{x}|H|\vec{x} \rangle$ have random values chosen according to some probability distribution. In this article I choose to use the Gaussian distribution

$$P(V) = \frac{1}{\sqrt{2\pi\sigma^2}} \exp\left(-\frac{V^2}{2\sigma^2}\right)$$

I call σ the disorder strength; this is related to the disorder strength used in the literature by a factor of $\sqrt{12}$ [16, 19].

At small disorder strengths, the Anderson model is dominated by its regular part; in particular the eigenvectors are extended throughout the whole system volume. However, there is a small but important departure from the ordered behavior: at the band edges one finds a few eigenvectors with volumes much smaller than the system volume. In fact, there is an energy E_{LOC} such that any eigenvector with eigenvalue E satisfying $|E| > E_{LOC}$ is localized. On average these eigenvectors decay exponentially with the spatial distance from their maximum[17]. As the disorder strength is increased, E_{LOC} gets smaller and smaller; i.e. more and more of the energy band becomes localized. At a critical disorder strength the whole energy band becomes localized. This phenomenon is called the Anderson transition; for the Gaussian probability distribution used in this paper it occurs at the critical disorder $\sigma_c = 6.149 \pm 0.006$ [16].

Note that these statements must all be understood as regarding the ensemble of Hamiltonians determined by the probabilistic distribution of the disorder: for instance, I am stating that above the critical disorder the subset of Hamiltonians with unlocalized eigenvectors is vanishingly small compared to the total ensemble size. Moreover, these statements are valid for an infinite lattice; the mapping to computations on a finite lattice is not always absolutely clear.

Studies of the locality of disordered systems have traditionally concentrated on computations of the Green's function, not the density matrix. It is expected that the average Green's function should decay exponentially as $\exp(-\frac{R}{\tilde{R}})$, where \tilde{R} is called the coherence length[5]. The density matrix, as we will see, is closely related to the Green's function, so one may hope that its average will also decay exponentially. However, there are two flies in the ointment: First, we do not need to know whether the average of all density matrices is localized, but instead whether each individual density matrix is localized. The difference between the two could be significant. Second, in a system below the critical disorder there will be unlocalized eigenvectors, and one might therefore expect the R^{-2} behavior typical of a metal.

Many $O(N)$ computations have treated systems which are disordered[22, 12, 26]. However, the $O(N)$ literature contains little theoretical material about the applicability of $O(N)$ algorithms to disordered systems. The originators of the "Locally Self-Consistent Green's Function" algorithm, which does not truncate the basis but instead does a sort of averaging

outside of a radius r , suggested that r is related to the coherence length[3], and also to the error induced by their averaging[4]. Zhang and Drabold computed the density matrix of amorphous Silicon using exact diagonalization and found an exponential decay[12]. In the next sections, I will show first theoretically and then numerically that $O(N)$ basis truncation algorithms are applicable to disordered systems, including ones far below the Anderson transition.

4. Estimating the Truncation Error

Basis truncation divides the basis into two projection operators, P_A for the part inside the localization cutoff R , and P_B for the part outside R . One can therefore divide the Hamiltonian H into two parts: $H_0 = P_A H P_A + P_B H P_B$ which leaves A and B disconnected, and a boundary term connecting A and B , $H_1 = P_A H P_B + P_B H P_A$. A basis truncation algorithm calculates $P_A f(H_0) P_A$. Therefore, estimating the error caused by basis truncation amounts to computing the effect of the boundary term H_1 on the matrix function $f(H)$. In the case of the density matrix, an exact equation for this boundary effect can be easily derived from the Dyson equation. First define the Green's functions $G(E) = (E - H)^{-1}$, $G_0(E) = (E - H_0)^{-1}$. Then note that the density matrix can be obtained from the Green's function through contour integration over the complex energy E : $\rho(\mu, T = 0, H) = 2\pi i \oint_{-\infty}^{\mu} G(E)$. Next, apply the Dyson equation $G = G_0 + G H_1 G_0$ twice to obtain:

$$G = G_0 + G_0 H_1 G_0 + G_0 H_1 G H_1 G_0$$

This gives an exact relation between the correct Green's function G of the untruncated Hamiltonian and the Green's function G_0 of the truncated Hamiltonian. In order to obtain a similar relation for the density matrix, one must make the poles in this expression explicit and then do a complex integration. Define $|a\rangle$ and $|b\rangle$ as two eigenvectors of H_0 which are both inside of the localization region, the set of $|c\rangle$ as the complete set of eigenvectors of H , and E_a , E_b , and E_c their respective energies. Then:

$$\langle a | (\rho(\mu) - \rho_0(\mu)) | b \rangle = \int_{-\infty}^{\infty} dE_c \langle a | H_1 | c \rangle \langle c | H_1 | b \rangle n(E_c) g(\mu, E_a, E_b, E_c)$$

where

$$g(\mu, E_a, E_b, E_c) = \oint_{-\infty}^{\mu} \frac{1}{E - E_a} \frac{1}{E - E_b} \frac{1}{E - E_c}$$

$n(E)$ is the spectral density $\sum_c \delta(E - E_c)$ and is often approximated as a continuous function.

Examining the integrated form of g with E_a, E_b, μ fixed and E_c free to vary, one finds that it changes sign at most once, and is well defined except when E_a or E_b is equal to μ . Its maximum is at $E_c = \mu$, where there is also a discontinuity. Because g is bounded and changes sign at most once, I feel free to approximate as follows:

$$\langle a | (\rho(\mu) - \rho_0(\mu)) | b \rangle \propto \overline{\langle a | H_1 | c \rangle \langle c | H_1 | b \rangle} \int_{-\infty}^{\infty} dE_c n(E_c) g(\mu, E_a, E_b, E_c)$$

where the overline denotes an average. (Note that if I were treating a system with lattice translational symmetry, the matrix elements would contribute an additional phase factor

depending on the Bloch momentum of the eigenvector $|c\rangle$. This phase factor can modify the results significantly, particularly in insulators. For simplicity I will ignore it in this discussion.)

At this point the problem has decoupled into two parts: estimation of the integral of ng , and estimation of the average matrix element. If one does the ng integral for a simple model where n is a constant n_0 inside the energy band and zero outside, one finds a result proportional to $\frac{n_0}{|E_a - E_b|}$ as long as μ is inside the energy band. (The integral is 0 outside the band because the truncated and untruncated density matrices are necessarily equal (zero or the identity) outside the band.) Remembering that g has its maximum value at $E_c = \mu$, I therefore make the following approximation:

$$\langle a|(\rho(\mu) - \rho_0(\mu))|b\rangle \propto \overline{\langle a|H_1|c\rangle\langle c|H_1|b\rangle} \frac{n(\mu)}{|E_a - E_b|}$$

The only remaining task is to estimate the average value of the transition matrix elements. These elements occur on the boundary between the sphere of radius R separating the localization region from the rest of the volume; their average will be determined by the average value of the eigenvectors on that sphere. More precisely, I approximate $\overline{\langle a|H_1|c\rangle} \propto 4\pi R^2 h \overline{|\langle a|R\hat{r}\rangle| |\langle R\hat{r}|c\rangle|}$, where h is some constant with units of energy times distance. I will consider three possibilities: extended eigenvectors with infinite coherence length, extended eigenvectors with finite coherence length, and localized eigenvectors.

4.1. Extended eigenvectors with infinite coherence length.

In this case the eigenvectors $|a\rangle$ and $|b\rangle$ in the truncated basis have normalization of order $\sqrt{\frac{3}{4\pi R^3}}$, and the eigenvectors $|c\rangle$ in the full basis have normalization of order $\sqrt{\frac{1}{N}}$. Therefore, the final result is:

$$\langle a|(\rho(\mu) - \rho_0(\mu))|b\rangle \propto \frac{n_R(\mu)}{|E_a - E_b|} \frac{h^2}{R^2}$$

$n_R(\mu) = n(\mu) \frac{4\pi R^3}{3N}$ is the spectral density within the truncation volume. Here we see the R^{-2} decay which is expected for metallic systems.

4.2. Extended eigenvectors with finite coherence length η .

I assume a very crude model of the incoherence where the eigenvector is broken into domains with constant phase, each domain of size $\frac{4\pi}{3}\eta^3$. The main effect is to decrease any integral over the eigenvector by a factor of $\sqrt{N_\eta}$, where N_η is the number of different domains where the integrand is non-zero. The surface of the truncation volume will intersect about $\frac{4\pi R^2}{4\pi\eta^2}$ such domains. Therefore if $R > \eta$,

$$\langle a|(\rho(\mu) - \rho_0(\mu))|b\rangle \propto \frac{n_R(\mu)}{|E_a - E_b|} \frac{h^2\eta^2}{R^4}$$

This is a very crude argument; possibly a better model of the finite coherence length would produce an even faster decay with R .

4.3. Localized eigenvectors.

I assume that the eigenvectors of both the truncated and untruncated system decay as $\exp(-\frac{r}{\tilde{R}})$, where \tilde{R} is the coherence length. Then if $R > \tilde{R}$ and both $|a\rangle$ and $|b\rangle$ are close

to the center of the truncation volume,

$$\langle a | (\rho(\mu) - \rho_0(\mu)) | b \rangle \propto \frac{n(\mu)}{|E_a - E_b|} \frac{h^2 R^4}{\tilde{R}^6} \exp\left(-\frac{2R}{\tilde{R}}\right)$$

5. Metrics

I make three types of measurements:

5.1. Matrix Comparisons

I compute the density matrix using both an $O(N)$ algorithm and an algorithm based on diagonalization of the Hamiltonian, and then compare the results. This requires a useful metric for comparing two matrices. First, note that the dot product used for comparing two vectors can be easily generalized to matrices:

$$MDP(A, B) \equiv \text{Tr}(AB) = \sum_{\vec{x}, \vec{y}} \langle \vec{x} | A | \vec{y} \rangle \langle \vec{x} | B | \vec{y} \rangle$$

If $A = B$, this matrix dot product is just the Frobenius norm, one of the traditional norms for matrices. Note also that matrix dot product is invariant under change of basis. Moreover, it is simple to show that $-1 \leq \frac{MDP(A, B)}{\sqrt{MDP(A, A)MDP(B, B)}} \leq 1$, so one may define the angle θ between two matrices as the arcsin of this quantity. Bowler and Gillan[24] justified this, showing that the concept of perpendicular and parallel matrices is valid and useful.

However the matrix dot product is not quite suited to my needs. $O(N)$ algorithms have a preferred, local basis, and thus are not well matched by a basis invariant measure. Moreover, the matrix functions which they compute are expected to agree best with the exact matrix functions close to the diagonal, and to agree not at all outside the truncation radius. Therefore, a more sensitive metric is needed, one that distinguishes different distances from the diagonal. I define the Partial Matrix Dot Product as:

$$MDP(A, B, \vec{x}) \equiv \sum_{\vec{y}} \langle \vec{y} | A | \vec{y} + \vec{x} \rangle \langle \vec{y} | B | \vec{y} + \vec{x} \rangle$$

The argument \vec{x} of this dot product allows me to obtain information about agreement at displacement \vec{x} from the diagonal. It is still valid to call this a dot product, because the magnitude of $\frac{MDP(A, B, \vec{x})}{\sqrt{MDP(A, A, \vec{x})MDP(B, B, \vec{x})}}$ is bounded by one, and thus one can compute a displacement-dependent angle $\theta(\vec{x})$ and relative magnitude $m(\vec{x})$. The partial matrix dot product has a simple sum rule relating it to the full matrix dot product: $MDP(A, B) = \sum_{\vec{x}} MDP(A, B, \vec{x})$.

In my results I actually compute another dot product, an angular average $MDP(A, B, r)$ over some, but not all, of the \vec{x} satisfying $r = |\vec{x}|$. (For $r \leq 3$ I used all such points, while for $r > 3$ I used only the axis and certain diagonals in order to reduce resource consumption.) When graphing the localization of the density matrix, I show:

$$\frac{MDP(A, A, r)}{MDP(A, A, 0)} \quad (1)$$

When graphing the angular error between two matrices, I show:

$$1 - \frac{MDP(A, B, r)}{\sqrt{MDP(A, A, r)MDP(B, B, r)}} = 2\sin^2\left(\frac{\theta(r)}{2}\right) \quad (2)$$

When graphing the error in matrix magnitude, I show:

$$\left| \frac{MDP(A, A, r)}{MDP(B, B, r)} - 1 \right| \quad (3)$$

5.2. Volumes

I use two measures of eigenvector volume. The first is the inverse of the first participation ratio; i.e. $\sum_{\vec{x}} |\langle \psi | \vec{x} \rangle|^2 / \sum_{\vec{x}} |\langle \psi | \vec{x} \rangle|^4$.

This quantity is a lattice friendly measure of volume because it has a minimum value of one when $|\psi\rangle$ is a delta function and a maximum value of the system size when $|\psi\rangle$ is a constant. However, if an eigenfunction consists of several isolated peaks its inverse first participation ratio may be still be small. Therefore, I also compute a second measure of the eigenvector's volume: $((2\pi)^D \det Q)^{-\frac{1}{2}}$, where Q is the second moment (or quadrupole tensor) of $|\langle \psi | \vec{x} \rangle|^2$.

5.3. Correlation Volumes

The third quantity of interest is the coherence volume of the eigenvectors. I obtained this quantity by first computing the correlation function $C(\vec{x}) = \int d\vec{k}^D |\langle \vec{k} | \psi \rangle|^2 \exp(i\vec{k} \cdot \vec{x})$, and then applying my two volume measures to $C^2(\vec{x})$.

6. Results

I studied ensembles of Anderson hamiltonia at disorder values of $\sigma = 0.65 + 0.5n$ ranging up to the the critical disorder $\sigma_c = 6.15$, and also at the larger disorder $\sigma = 9.15$. A truncation radius of $R = 5$ was used uniformly. A lattice size of 16^3 was used, and calculations with 12^3 and 20^3 lattices at the critical disorder σ_c indicate that finite size effects are small. The largest such effect is an improvement of the basis truncation algorithm's accuracy at smaller lattice volumes. At each disorder I calculated the density matrix at 13 values of the Fermi level μ ranging uniformly from -12 to 12 , which covered the whole energy band at the lower disorders, and most of it even at larger disorders.

A low temperature ($T = 0.05$) was chosen in order to minimize any temperature effect. A careful examination of the density matrix's behavior at $\mu = 0$ showed that any temperature effect was swamped by other effects. In particular, at low disorder the density matrix's behavior is dominated by lattice effects. Because of the low temperature a large number of Chebyshev terms was needed; for all thirteen ensembles I used 500 terms, but in nine of them I repeated the calculations with 1000 terms.

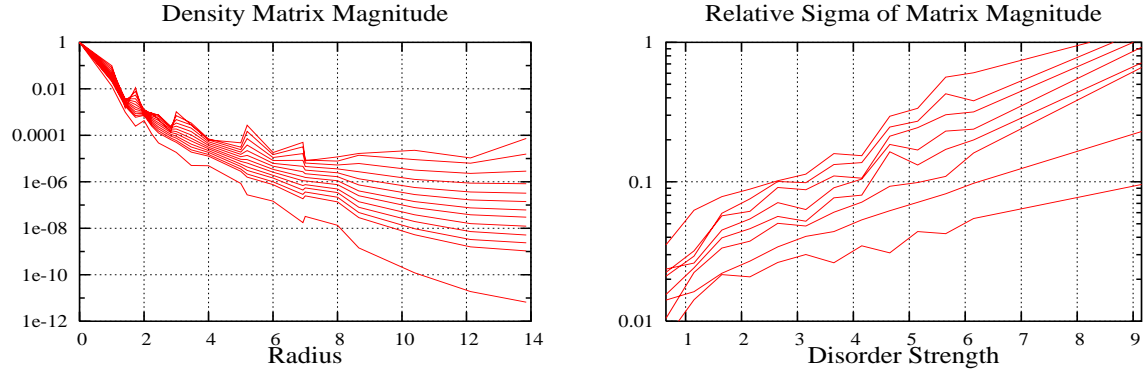


Figure 1 shows the density matrix magnitude (see equation 1) at $\mu = 0$. Each line corresponds to a different disorder strength; lower disorders are higher on the graph. For $r > 0$ and $\sigma \geq 1.65$ a good fit can be obtained by $MDP(\rho, \rho, r) \propto r^{-4} \exp(-\frac{2r}{\tilde{R}})$, where the coherence length is given by $\tilde{R} = ((0.044\sigma) - 0.049)^{-1}$. Note the almost inverse relation between the coherence length \tilde{R} and the disorder strength σ . The second constant 0.049 in the parenthesis actually decreases significantly for large σ , but is kept as a constant here for simplicity. Lattice effects cause a systematic fitting uncertainty in the first constant 0.044 of roughly 10%. Similar fits can be obtained at other Fermi levels within the band $|\mu| \leq 6$; the first constant has a minimum at $\mu = 2$ and a total variation of about 20%, while the second constant varies a lot, including a rapid decrease above $\mu = 0$. Outside $|\mu| \leq 6$ the density matrix magnitude drops off very rapidly and the above fit doesn't work well.

Now I consider the statistical distribution of the density matrix magnitude. Figure 2 shows the ratio of the second moment to the mean, again at $\mu = 0$. The different lines correspond to different radii $r = n\sqrt{3}$, with smaller radii lower on the graph. Note that this ratio seems to grow roughly exponentially with the disorder σ . An examination of the kurtosis of the density matrix magnitude shows that for $\sigma \geq 5.15$ this quantity becomes very large, starting at larger radii and larger Fermi level $|\mu|$. These statistics indicate that at the Anderson transition the statistical distribution of the density matrix magnitude develops a long tail; it loses its self-averaging property.

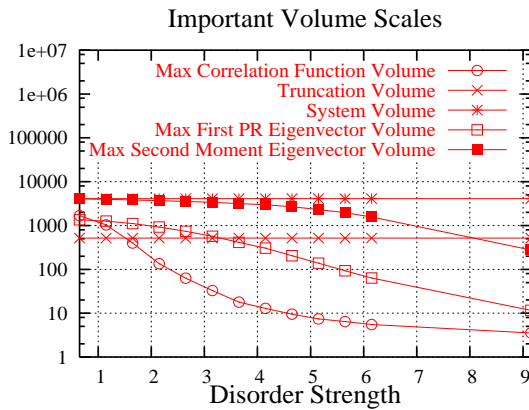
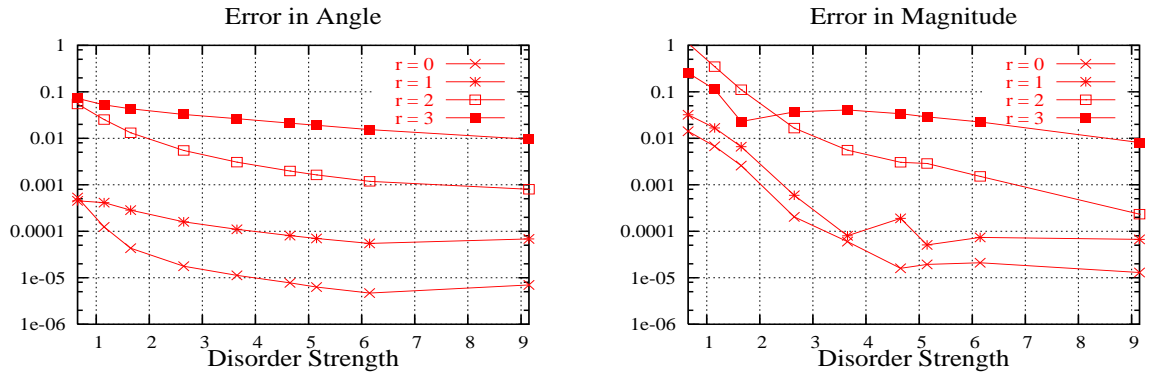


Figure 3 shows the important volume scales in this problem as a function of disorder σ . The volume of the eigenvectors, as measured via the second moment, remains large even at large disorders. This is due to the fact that states with similar energies will mix even if they are connected by exponentially small matrix elements. However, mixing caused by such small matrix elements does not influence the density matrix, because it essentially just induces a unitary transformation of the mixed eigenvectors, and as we know the density matrix is invariant under unitary transformations. It is more instructive to look at the inverse of the first participation ratio. This volume becomes significantly smaller than the truncation volume in the range $\sigma = 3.15$ to $\sigma = 4.15$.

Figure 3 also shows the maximum value of the coherence volume; $V_C = \max_E V(E)$. Note that it becomes small much sooner than the eigenvector volume, in the range from $\sigma = 1.65$ to $\sigma = 2.15$. For $\sigma \geq 1.15$ and $V_C \gg 1$ the coherence volume is roughly proportional to σ^{-3} . This fits well with the density matrix's coherence length at large σ , but not at small σ .



Figures 4 and 5 show the $O(N)$ algorithm's angular error (see eq. 2) and error in magnitude (eq. 3) as a function of disorder. Again the Fermi level μ is 0. At disorder strengths $\sigma > 2.15$ their behavior is roughly independent of the Fermi level μ , with two exceptions. Firstly, if $\sigma \geq 4.65$ and r is small, the errors decrease as $|\mu|$ grows large. Secondly, as μ increases the $r = 0$ angular error decreases rapidly. Recall that the Chebyshev approximation's error is controlled by the factor ST/Δ where Δ is the band gap; the bend in the $r = 0, 1$ error lines around $\sigma_c = 6.15$ is likely attributable to the widening of the band width of at higher disorders; in fact the errors start getting worse at $\sigma \approx 4.15$ already in computations with only 500 coefficients.

The $O(N)$ algorithm begins to work well at $r = 0, 1$ at quite small disorders, and the $r = 2$ error falls to 1% at about $\sigma = 3.15$. Apparently the $O(N)$ algorithm's success is controlled by the coherence volume, not by the eigenvector volumes. Therefore a good rule of thumb for evaluating the applicability of an $O(N)$ algorithm is to find the system's coherence volume. How to do that reliably? Probably the best way is to compute some eigenvectors and look at the volume of individual peaks of the correlation function. However, one must remember that different parts of the spectrum show different coherence volumes; in fact at disorder strengths $\sigma \leq 6.15$ the coherence length shows two peaks at energies $|E| = 6 - 8$. At $\sigma \leq 1.65$, the peaks are a factor of 10 above the minimum. Therefore some judgement is required in finding a suitable eigenvector. An alternative might be to use the Coherent Potential Approximation[25] to estimate the coherence length; I have yet to check its agreement with the data presented

here.

7. Reliability of These Results

I have already discussed the errors due to the finite lattice size. I have also mentioned that fact that my matrix dot product $MDP(A, B, r)$ omitted many angles outside of the radius $r = 3$; the errors due to this approximation are hard to estimate but are expected to be small because the Anderson model does not possess any rotational symmetry. Comparison of calculations with 500 and 1000 Chebyshev coefficients show identical results at $\sigma \leq 3.65$, and indicate that the only risk at higher disorder strengths is an overestimate of the error. The main risks to the results of this paper probably lie in two areas: finite ensemble size, and software reliability and reproducibility. I have taken steps to manage both issues:

7.1. Finite ensemble size.

Most ensembles consisted of 33 realizations, but several (at $\sigma = 1.15, 6.15, 9.15$) contained 100 realizations. Graphing any quantity across several disorders, one immediately notices that there is little noise induced overlap of the two graphs. At the critical disorder the same quantities were computed with three different lattice sizes (100 realizations at both 12^3 and 16^3 , and 10 realizations at 20^3), and the agreement is very good. The sigma and kurtosis of the MDP-based observables were also measured. The size of the sigma relative to the signal is usually quite small (especially compared to the signal variation over many orders of magnitude.) The kurtosis was generally well within the interval that occurs with probability 10^{-5} or better in a normal distribution. At higher disorders there were some exceptions with high kurtosis, but remarkably the pattern of high kurtosis was identical on the 12^3 and 16^3 lattices. Therefore, it seems likely that risks due to finite ensemble size are under control.

7.2. Software Reliability and Reproducibility.

I have tried very hard to reduce this risk. The software includes an automated test suite which tests all computational functions except the highest level output (graph printing) routines. Moreover, I have taken pains to enable other researchers to easily reproduce and check my results, simply by installing my software, compiling it with the GNU gcc compiler[28] and starting it running. The software, with all needed configuration files, will be made available under the GNU Public License[27]; check www.sacksteder.com for further details.

ACKNOWLEDGEMENTS

Special thanks to my advisor, Giorgio Parisi, for his attentiveness, stimulation, and encouragement. Thank you also to Stephan Goedecker for sharing one of his $O(N)$ codes, to the OXON group for sharing their code (though it remained unused), and to the organizers of the 21st International Workshop on Numerical Linear Algebra and its Applications for putting that event together.

REFERENCES

1. Ordejon P. Order-N tight-binding methods for electronic structure and molecular dynamics. *Computational Materials Science* 1998; **12**:157–191.
2. Scuseria GE. Linear scaling density functional calculations with gaussian orbitals. *Journal of Physical Chemistry A* 1999; **103**(25):4782–4290.
3. Abrikosov IA, Niklasson AMN, Simak SI, Johansson B, Ruban AV, Skriver HL. Order-N Green's function technique for local environment effects in alloys. *Physical Review Letters* 1996; **76**(12):4203–4206.
4. Abrikosov IA, Simak SI, Johansson B, Ruban AV, Skriver HL. Locally self-consistent Green's function approach to the electronic structure problem. *Physical Review B* 1997; **56**(15):9319–9334.
5. Economou EN, Soukoulis CM, Zdetsis AD. Locally self-consistent Green's function approach to the electronic structure problem. *Physical Review B* 1984; **36**(4):1686–1694.
6. Baer R, Head-Gordon M. Sparsity of the density matrix in Kohn-Sham density functional theory and an assessment of linear system-size scaling methods. *Physical Review Letters* 1997; **79**(20):3962–3965.
7. Baer R, Head-Gordon M. Chebyshev expansion methods for electronic structure calculations on large molecular systems. *Journal of Chemical Physics* 1997; **107**(23):10003–10013.
8. Goedecker S. Decay properties of the finite-temperature density matrix in metals. *Physical Review B* 1998; **58**(7):3501–3502. arXiv:cond-mat/9804013.
9. Ismail-Beigi S, Arias T. Locality of the density matrix in metals, semiconductors, and insulators. *Physical Review Letters* 1999; **82**(10):2127–2130.
10. Goedecker S, Ivanov OV. Frequency localization properties of the density matrix and its resulting hypersparsity in a wavelet representation. *Physical Review B* 1999; **59**(11):7270–7273.
11. Goedecker S. Linear scaling electronic structure methods. *Reviews of Modern Physics* 1999; **71**(4):1085–1123.
12. Zhang X, Drabold DA. Properties of the density matrix from realistic calculations. *Physical Review B* 2001; **63**(23):233109–233112.
13. Koch E, Goedecker S. Locality properties and Wannier functions for interacting systems. *Solid State Communications* 2001; **119**:105–109. arXiv:cond-mat/0105401.
14. He L, Vanderbilt D. Exponential decay properties of Wannier functions and related quantities. *Physical Review Letters* 2001; **86**(23):5341–5344. arXiv:cond-mat/0102016.
15. Taraskin SN, Fry PA, Zhang X, Drabold DA, Elliott SR. Spatial decay of the single-particle density matrix in tight-binding models: analytic results in two dimensions. *Physical Review B* 2002; **66**(23):233101–233104.
16. Slevin K, Ohtsuki T. Numerical verification of universality for the Anderson transition. *Physical Review B* 2001; **63**(4):45108–45112. arXiv:cond-mat/0101272.
17. Kantelhardt JW, Bunde A. Sublocalization, superlocalization, and violation of standard single-parameter scaling in the Anderson model. *Physical Review B* 2002; **66**(3):35118–35128. arXiv:cond-mat/0201356.
18. Anderson PW. Absence of diffusion in certain random lattices. *Physical Review* 1958; **109**(5):1492–1505.
19. Bulka B, Schreiber M, Kramer B. Localization, quantum interference, and the metal-insulator transition. *Zeitschrift fur Physik B: Condensed Matter* 1987; **66**:21–30.
20. Resta R. Why are insulators insulating and metals conducting? *Journal of Physics: Condensed Matter* 2002; **14**:R625–R626.
21. Yang W. Direct calculation of electron density in density-functional theory. *Physical Review Letters* 1991; **66**(11):1438–1441.
22. Goedecker S, Colombo L. Efficient linear scaling algorithm for tight-binding molecular dynamics. *Physical Review Letters* 1994; **73**(1):122–125.
23. Goedecker S, Teter M. Tight-binding electronic structure calculations and tight-binding molecular dynamics with localized orbitals. *Physical Review B* 1995; **51**(15):9455–9464.
24. Bowler DR, Gillan MJ. Density matrices in O(N) electronic structure calculations: theory and applications. *Computer Physics Communications* 1999; **120**(2-3):95–108. arXiv:cond-mat/9810042.
25. Soven P. Coherent-Potential model of substitutional disordered alloys. *Physics Review* 1967; **156**:809–813.
26. Schubert G, Weisse A, Fehske H. Comparative numerical study of localization in disordered electron systems. <http://arxiv.org> 2003; **arXiv:cond-mat/0309015**. [28 November 2003].
27. Licenses. <http://www.gnu.org/licenses/licenses.html> [28 November 2003].
28. Welcome to the GCC home page! <http://www.gnu.org/software/gcc/gcc.html> [28 November 2003].